Free Radical Biology and Medicine 63 (2013) 222–234

Contents lists available at SciVerse ScienceDirect

Free Radical Biology and Medicine

journal homepage: www.elsevier.com/locate/freeradbiomed

Original Contribution

SIRT3 deacetylates FOXO3 to protect mitochondria against oxidative damage

Anne H.H. Tseng [a,b,c], Shyan-Shu Shieh [c], Danny Ling Wang [b,c,d,*]

[a] Institute of Biochemistry and Molecular Biology, School of Life Sciences, National Yang-Ming University, 11221 Taipei, Taiwan
[b] Taiwan International Graduate Program, Molecular Medicine Program, Academia Sinica, 11529 Taipei, Taiwan
[c] Institute of Biomedical Sciences, Academia Sinica, 11529 Taipei, Taiwan
[d] Institute of Medical Sciences, Tzu-Chi University, 97004 Hualien, Taiwan

ARTICLE INFO

Article history:
Received 14 December 2012
Received in revised form
1 May 2013
Accepted 1 May 2013
Available online 7 May 2013

Keywords:
SIRT3
FOXO3
Mitochondrial homeostasis
Mitochondrial biogenesis
Mitochondrial fission/fusion
Mitophagy
Aging
Oxidative stress
Free radicals

ABSTRACT

Progressive accumulation of defective mitochondria is a common feature of aged cells. SIRT3 is a NAD^+-dependent protein deacetylase that regulates mitochondrial function and metabolism in response to caloric restriction and stress. FOXO3 is a direct target of SIRT3 and functions as a forkhead transcription factor to govern diverse cellular responses to stress. Here we show that hydrogen peroxide induces SIRT3 to deacetylate FOXO3 at K271 and K290, followed by the upregulation of a set of genes that are essential for mitochondrial homeostasis (mitochondrial biogenesis, fission/fusion, and mitophagy). Consequently, SIRT3-mediated deacetylation of FOXO3 modulates mitochondrial mass, ATP production, and clearance of defective mitochondria. Thus, mitochondrial quantity and quality are ensured to maintain mitochondrial reserve capacity in response to oxidative damage. Maladaptation to oxidative stress is a major risk factor underlying aging and many aging-related diseases. Hence, our finding that SIRT3 deacetylates FOXO3 to protect mitochondria against oxidative stress provides a possible direction for aging-delaying therapies and disease intervention.

Progressive accumulation of defective mitochondria in cells is tightly linked to the decrease in physiologic function that occurs during aging and to the pathologies of aging-related diseases, such as cancer, Parkinson disease, type 2 diabetes, and cardiovascular disease [1–3]. To date, caloric restriction (CR) is the most effective means to delay aging and aging-related diseases in various organisms. The activation of sirtuins (SIRTs), NAD^+-dependent deacetylases, is central to the beneficial effects of CR [1,4].

Humans express seven SIRTs, which share a common 275-amino-acid catalytic domain and target a variety of substrates to coordinate diverse actions in cellular metabolism, genomic integrity, and stress resistance [4,5]. SIRT3 is localized in mitochondria and serves as a primary regulator of mitochondrial protein acetylation [5,6]. SIRT3-knockout mice exhibit cardiac hypertrophy, whereas transgenic mice that overexpress SIRT3 are cardioprotected from hypertrophic stimuli [7]. The expression of SIRT3 is induced by CR or oxidative stress. It facilitates the deacetylation of a number of proteins that coordinate diverse actions in cellular metabolism, genomic integrity, stress resistance, and tumor suppression [8–12]. In response to CR, SIRT3 deacetylates a number of mitochondrial proteins, including manganese superoxide dismutase, which is responsible for limiting the accumulation of reactive oxygen species (ROS) [9]; isocitrate dehydrogenase 2, which enhances the glutathione antioxidant defense system [10]; and acyl coenzyme A dehydrogenase, which is involved in mitochondrial fatty-acid oxidation [11]. SIRT3 is also induced by oxidative stress to deacetylate Ku70, which protects cells from Bax-mediated cell death [12].

The SIRT3 substrate forkhead box O3 (FOXO3) is a forkhead transcription factor that mediates the expression of multiple genes that govern cellular development, differentiation, survival, apoptosis, stress resistance, metabolism, autophagy, and longevity [13–15]. SIRT3-mediated deacetylation of FOXO3 reduces levels of cellular ROS by upregulating the antioxidant enzymes manganese superoxide dismutase and catalase, which further ameliorates cardiac hypertrophy in mice [7,16].

Our understanding of the molecular events that underlie SIRT3-mediated deacetylation of FOXO3 is, however, limited. Moreover, little is known about whether the interaction of these proteins contributes to the mitochondrial protection processes in response to oxidative stress.

In this study, we found that SIRT3 was induced by hydrogen peroxide to deacetylate FOXO3 at K271 and K290. This deacetylation drives the expression of multiple FOXO3-dependent genes

Abbreviations: BAEC, bovine aortic endothelial cell; CR, caloric restriction; EC, endothelial cell; HUVEC, human umbilical vein endothelial cell; OCR, oxygen consumption rate; ROS, reactive oxygen species.

* Corresponding author at: Institute of Biomedical Sciences, Academia Sinica, 11529 Taipei, Taiwan. Fax: +886 2 2782 9143.
E-mail address: lingwang@ibms.sinica.edu.tw (D.L. Wang).

0891-5849/$ - see front matter © 2013 Elsevier Inc. All rights reserved.
http://dx.doi.org/10.1016/j.freeradbiomed.2013.05.002

that are indispensable for mitochondrial homeostasis. Mitochondrial homeostasis maintains mitochondrial function and integrity through the generation of new mitochondria (mitochondrial biogenesis) and the selective degradation of defective mitochondria (mitophagy); it is coupled with mitochondrial fusion/fission [2,17]. Our results demonstrate that SIRT3–FOXO3 upregulate PGC-1α and TFAM to promote mitochondrial biogenesis; induce Drp1, Fis1, and Mfn2 to coordinate mitochondrial fission/fusion; and increase Bnip3, Nix, and LC3-II/LC3-I to execute mitophagy under oxidative stress. As such, the SIRT3–FOXO3 cascade significantly improves mitochondrial quantity and quality, which helps to preserve the mitochondrial reserve capacity, thereby protecting cells from oxidative damage.

Materials and methods

Cell culture

Human umbilical vein endothelial cells (HUVECs) were obtained from Cell Applications, Inc. HUVECs were cultured in M199 medium (GIBCO) supplemented with 100 U/ml penicillin/streptomycin (GIBCO), 2.5 μg/ml amphotericin B (GIBCO), 20% fetal bovine serum (FBS; HyClone), and 20% endothelial cell (EC) growth medium (Lonza). HUVECs from passages 3–6 were used in experiments.

Bovine aortic ECs (BAECs) were isolated from fresh bovine bronchoesophageal artery by treatment with 0.01% collagenase type I (Sigma) in phosphate-buffered saline (PBS) for 20 min at 37 °C. BAECs were isolated by fluorescence-activated cell sorting with 1,1′-dioctadecyl-L-3,3,3′,3′-tetramethylindocarbocyanine perchlorate (Biomedical Technologies) and cultured in low-glucose Dulbecco's modified Eagle medium (DMEM; GIBCO) supplemented with 100 U/ml penicillin/streptomycin and 10% FBS. BAECs from passages 12 to 16 were used in experiments.

Constructs

Human SIRT3 cDNA (NM_012239.5) was kindly provided by Dr. Chun-Hua Hsu (National Taiwan University, Taiwan) and inserted into the EcoRI/XhoI site of the vector pIRES-hrGFP-1a (Stratagene), which includes three contiguous Flag epitopes. The dominant-negative mutant of SIRT3 (H248Y) was generated using the QuickChange site-directed mutagenesis kit (Stratagene) with the following mutagenic primers: H248Y-F, 5′-TCAAAGCTGGTTGAAGCTTACGGAACCTTTGCCTCTGCC-3′, and H248Y-R, 5′-GGCAGAGGCAAAGGTTCCGTAAGCTTCAACCAGCTTTGA-3′. The human FOXO3–enhanced green fluorescent protein (EGFP) expression plasmid was kindly provided by Dr. Wei-Chien Huang (China Medical University, Taiwan). The constitutively acetylated and deacetylated mutants of FOXO3 (K271/290Q and K271/290R) were created using the QuickChange site-directed mutagenesis kit ;with the following mutagenic primers: K271Q-F, 5′-GGCCGCGCAGCCAAGAAGCAAGCAGCCCTGCAGACAGCC-3′; K271Q-R, 5′-GGCTGTCTGCAGGGCTGCTTGCTTCTTGGCTGCGCGGCC-3′; K290Q-F, 5′-AGTCCCTCCCAGCTCTCCCAATGGCCTGGCAGCCCCACG-3′; K290Q-R, 5′-CGTGGGGCTGCCAGGCCATTGGGAGAGCTGGGAGGGACT-3′; K271R-F, 5′-GGCCGCGCAGCCAAGAAGAGAGCAGCCCTGCAGACAGCC-3′; K271R-R, 5′-GGCTGTCTGCAGGGCTGCTCTCTTCTTGGCTGCGCGGCC-3′; K290R-F, 5′-AGTCCCTCCCAGCTCTCCAGATGGCCTGGCAGCCCCACG-3′; and K290R-R, 5′-CGTGGGGCTGCCAGGCCATCTGGAGAGCTGGGAGGGACT-3′. All constructs were verified by DNA sequencing.

Transfection

For small interfering RNA (siRNA) transfection, SIRT3 or control ON-TARGETplus SMARTpool siRNA (Thermo Scientific) and Lipofectamine 2000 (Invitrogen) were used. For DNA plasmid transfection, TurboFect (Fermentas) was used.

Protein extraction, immunoprecipitation, and immunoblotting

Cells were lysed in 50 mM Tris–HCl (pH 7.4; Merck) containing 150 mM NaCl (Merck), 0.25% deoxycholic acid (Sigma), 1% (v/v) NP-40 (Sigma), 1 mM EDTA (Merck), 20 mM NaF (Sigma), 10 mM sodium pyrophosphate (Sigma), 10 mM glycerol 3-phosphate (Sigma), 1 mM sodium orthovanadate (Sigma), 1 mM nicotinamide (Sigma), 1 μM trichostatin A (Sigma), and protease inhibitor cocktail (Roche Applied Science). After sonication, the suspension was centrifuged at 10,000*g* at 4 °C for 15 min, and the resulting protein concentration of the supernatant was determined by the BCA protein assay kit (Thermo Scientific). Total protein (1.5 mg) was incubated with anti-FOXO3 (Santa Cruz Biotechnology) or anti-Flag (Sigma) for 3 h at 4 °C. Then, 50 μl of precleared protein G–Sepharose (Thermo Scientific) was added and incubated at 4 °C overnight. The resulting immunoprecipitate was boiled with 35 μl of SDS reducing sample buffer and used for immunoblotting. The proteins were subjected to 9 or 14% SDS–polyacrylamide gel electrophoresis and were then transferred to polyvinylidene difluoride membranes that were blocked with TBST (20 mM Tris–HCl, pH 7.5; 150 mM NaCl; 0.1% (v/v) Tween 20) containing 5% bovine serum albumin (BSA). Membranes were probed with the appropriate primary antibodies for 3 h at room temperature, washed with TBST, incubated with horseradish peroxidase-conjugated anti-mouse or anti-rabbit antibody (1:20,000; Chemicon) for 3 h at room temperature, and then washed with TBST. Immunoreactive bands were visualized using Immobilon Western chemiluminescent HRP substrate (Millipore) or Supersignal West Femto chemiluminescent substrate (Thermo Scientific) with the Luminescent image analyzer (LAS-3000; Fujifilm). Details about the primary antibodies are provided below.

Subcellular fractionation

Cell fractionation into cytosolic, nuclear, and mitochondrial fractions was performed by a variation of a published protocol [18]. Briefly, 8×10^6 cells were scraped into 10 ml of grinding medium (250 mM sucrose, pH 7.4; 2 mM EDTA; 1 mg/ml BSA; protease inhibitor cocktail) and collected by centrifugation at 800*g* at 4 °C for 5 min. The pellet was resuspended in 1 ml of grinding medium, gently sonicated, and centrifuged at 800*g* at 4 °C for 12 min. The pellet was kept on ice for nuclear protein extraction, and the supernatant was immediately centrifuged at 8500*g* at 4 °C for 20 min. The resulting supernatant contained the cytosolic fraction. The pellet was resuspended in 100 μl of buffer S (150 mM sucrose, pH 7.4; 40 mM KCl; 25 mM Tris–HCl; 1 mg/ml BSA; 2% Chaps; protease inhibitor cocktail), vigorously sonicated, and then centrifuged at 10,000*g* at 4 °C for 20 min. The resulting supernatant contained the mitochondrial fraction. The nuclear pellet was resuspended in 500 μl of buffer A (10 mM Hepes, pH 7.9; 10 mM KCl; 0.1 mM $MgCl_2$; 0.1 mM EDTA; 0.1 mM dithiothreitol (DTT); 0.05% NP-40; protease inhibitor cocktail), incubated on ice for 10 min, and centrifuged at 500*g* at 4 °C for 10 min. The pellet was then extracted with 200 μl of buffer B (10 mM Hepes, pH 7.9; 100 mM NaCl; 1.5 mM $MgCl_2$; 0.1 mM EDTA; 0.1 mM DTT; protease inhibitor cocktail). After vigorous sonication, samples were centrifuged at 10,000*g* at 4 °C for 20 min. The resulting supernatant contained the nuclear fraction. All supernatants were boiled in SDS reducing sample buffer, and 40 μl of the cytosolic

fraction, 20 μl of the nuclear fraction, and 20 μl of the mitochondrial fraction were separated by 9% SDS–polyacrylamide gel electrophoresis and analyzed by immunoblotting.

Details of antibodies used in immunoblotting analysis

Antibodies to the following proteins were used: acetyllysine (1:250) and LC3 (1:1000; LC3-I 19 kDa, LC3-II 17 kDa) from Cell Signaling Technology; SIRT3 (1:250; long-form SIRT3 45 kDa, short-form SIRT3 30 kDa) from Abgent; EGFP (1:1000), FOXO3 (1:1000; 95 kDa), actin (1:3000; 42 kDa), tubulin (1:3000; 55 kDa), and PGC-1α (1:500; 92 kDa) from Santa Cruz Biotechnology; Flag (1:3000) from Sigma; TFAM (1:1000; 29 kDa) from Abcam; Fis1 (1:1000; 17 kDa), Mfn2 (1:1000; 86 kDa), Bnip3 (1:1000; 22 kDa), and Nix (1:1000; 40 kDa) from GeneTex; and Drp1 (1:3000; 80 kDa) from Novus.

Statistical analysis for immunoblot data

The intensity of bands in Western blots was quantified using MetaMorph software (Universal Imaging) or NIH Image/ImageJ. The intensity value for each protein was normalized against the intensity of the tubulin or actin band for that same sample. The values after normalizing to tubulin or actin in the control samples were set as 1. All values are expressed as the mean ± the standard error of the mean (SEM) and were analyzed using a Student *t* test with two-tailed distribution between groups as indicated in the graphs. All calculations were performed by Microsoft Excel.

Mitochondrial mass measurement

Cells (1×10^6) from each experimental condition were serum-starved in DMEM with 2% FBS overnight and then stained with MitoTracker Deep Red FM (20 nM in DMEM+2% FBS). After 30 min, the cells were washed with PBS, trypsinized, collected, and filtered through 35-μm nylon mesh, which is incorporated into the tube cap (BD Biosciences). Stained cells were analyzed immediately with an LSR II flow cytometer (BD Biosciences). All gain and amplifier settings were held constant for the duration of measurement. Ten thousand events were characterized and recorded by FACS Diva software.

Intracellular ATP measurement

Cells from each experimental condition were trypsinized, collected, and counted with a Countess automated cell counter (Invitrogen). Equal numbers of viable cells (2.5×10^5) from each treatment were assessed in an ATP assay using the ATP Bioluminescence Assay Kit HS II (Roche).

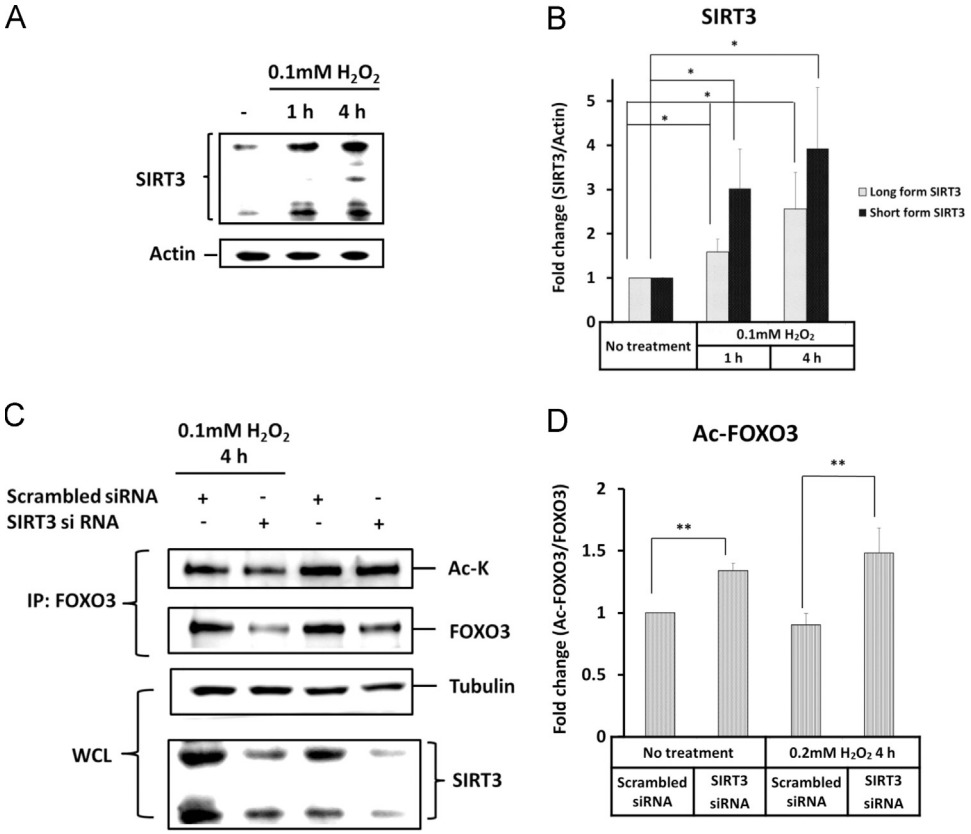

Fig. 1. SIRT3 is induced by hydrogen peroxide to deacetylate FOXO3. (A) Effects of hydrogen peroxide on the expression levels of SIRT3. HUVECs were treated with 0.1 mM hydrogen peroxide for 1 and 4 h; control cells were untreated (–). Total proteins were analyzed by immunoblotting for SIRT3 and actin. (B) Densitometric analysis of the immunoblotting results in (A) showing that hydrogen peroxide increases expression of both the long and the short forms of SIRT3. (C) Effects of SIRT3 on FOXO3 acetylation in response to hydrogen peroxide treatment. HUVECs were treated with a scrambled siRNA (control) or SIRT3 siRNA, immunoprecipitated with FOXO3 antibody, and analyzed by immunoblotting. (D) Densitometric analysis of the immunoblotting results in (C) showing that SIRT3 deacetylates FOXO3 in response to hydrogen peroxide treatment. All values are the mean ± SEM of the results from three independent experiments. Statistical analyses were performed by Student's *t* test between groups as indicated in the graphs. $^{*}p < 0.05$; $^{**}p < 0.01$.

Immunofluorescence confocal microscopy

BAECs (4×10^6) were transfected with 10 μg of DNA constructs. One day after transfection, 1.5×10^5 cells were plated onto fibronectin-coated coverslips (18 mm in diameter) in a 24-well culture dish. After 6 h, the cells were serum-starved in DMEM with 2% FBS overnight. Normal cells were stained for 30 min with MitoTracker Deep Red FM (100 nM in DMEM+2% FBS) before fixation. Mitochondria in hydrogen peroxide-treated cells were identified by overexpression of pDsRed2-Mito (Clontech) before fixation or stained with primary antibodies against Tom 20 (1:200; Santa Cruz Biotechnology) after fixation. All cells were fixed with 4% paraformaldehyde in PBS for 15 min, permeabilized with 0.5% Triton X-100 in PBS for 30 min, and blocked with 5% goat serum in PBS for 1 h. Cells were then incubated with primary antibodies against Flag (1:200; Sigma), hemagglutinin (HA; 1:200; Santa Cruz Biotechnology), p62 (1:200; GeneTex), or Lamp1 (1:200; Santa Cruz Biotechnology) at 4 °C overnight, followed by Alexa Fluor 350-, Alexa Fluor 594-, or Alexa Fluor 633-conjugated goat anti-mouse or anti-rabbit antibody (1:500; Invitrogen) at room temperature for 3 h and then mounted in ProLong Gold (Invitrogen). Fluorescence images were obtained using an inverted confocal fluorescence microscope (Zeiss LSM510) with a 100× oil-immersion objective (EC Plan-Neofluar 100 × /1.3 Oil Ph3). Fields were selected at random, and 100 cells were counted in total from three independent experiments. Images were acquired using Zeiss LSM Image Browser software.

Bioenergetic measurements

An XF24 extracellular flux analyzer (Seahorse Bioscience) was used to determine the metabolic characteristics of cells. BAECs were cotransfected with siRNA and DNA constructs using Lipofectamine 2000 (Invitrogen). After 24 h, the cells were seeded at a density of 50,000 cells/well on XF24 tissue culture plates. After a 5-h incubation, adherent cells were treated with 0.2 mM hydrogen peroxide in DMEM with 2% FBS for 14 h. Before the assay, the culture medium was changed to sodium bicarbonate-free DMEM with 2% FBS for 2 h in a CO_2-free incubator. The oxygen consumption rate (OCR) was measured under basal conditions or in the presence of 3 μM oligomycin (an inhibitor of oxidative phosphorylation) or 1 μM carbonyl cyanide 4-(trifluoromethoxy)phenylhydrazone (a mitochondrial uncoupler) or 3 μM antimycin A (an inhibitor of complex III). Three successive 3-min measurements were performed with intermeasurement mixing. All OCR values were recorded and the area under the curve (AUC) for each sample was calculated before and after each drug injection. For statistical analysis, the Student *t* test was performed between groups as indicated in the graphs. Under all experimental conditions, four independent experiments were analyzed, and *p* values are noted in the figures.

Results

Hydrogen peroxide induces SIRT3 to deacetylate FOXO3

ECs that line the interior surface of blood vessels are exposed to widely varying stimuli in the vasculature. The ECs used in this study can serve as an in vitro model for vascular aging and vascular pathogenesis in higher order biological species [19,20]. We examined whether the expression of aging-related SIRT3 is modulated by oxidative stress in HUVECs. SIRT3 is expressed in two forms in mammalian cells, a long form (~44 kDa) and a short form (~28 kDa) [7]. When HUVECs were treated with 0.1 mM hydrogen peroxide for 1 and 4 h, the levels of both SIRT3 forms increased in a time-dependent manner in contrast to the untreated controls (Figs. 1A and B). We then examined whether the acetylation of the SIRT3 substrate, FOXO3, is also modulated by

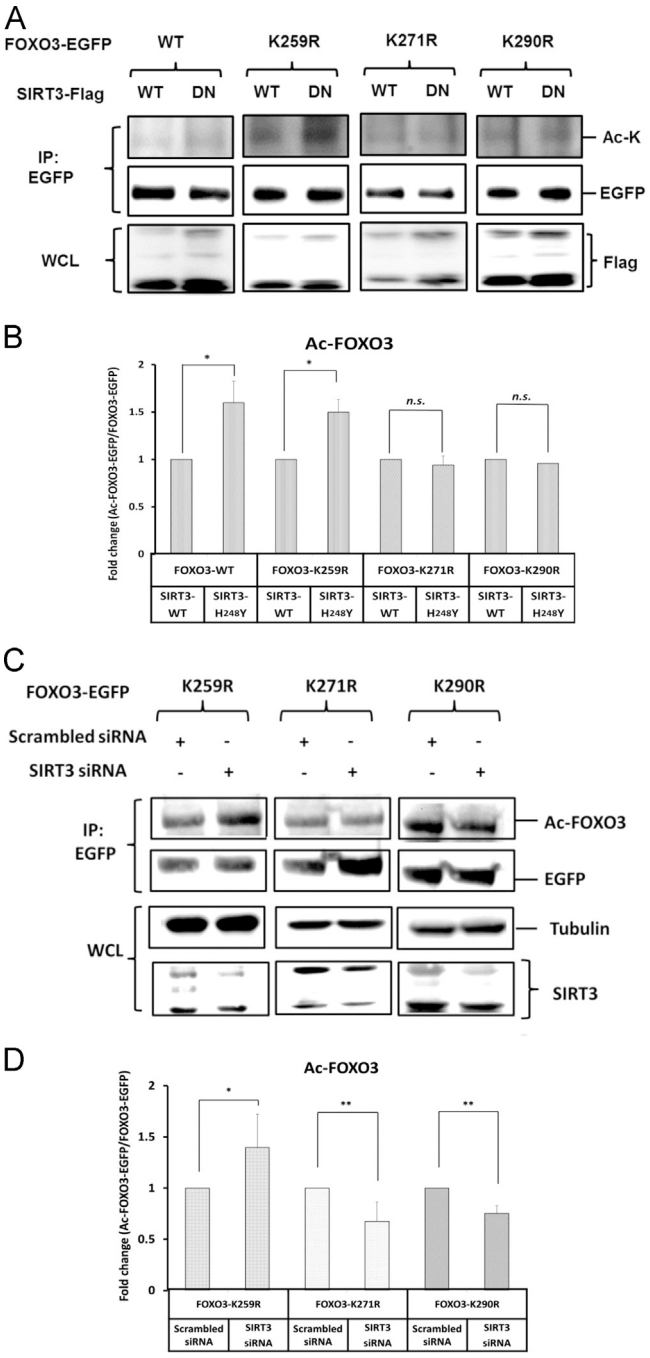

Fig. 2. SIRT3 deacetylates FOXO3 at K271 and K290. (A) Levels of FOXO3 acetylation in BAECs that overexpressed Flag-tagged $SIRT3^{WT}$ or $SIRT3^{H248Y}$, together with EGFP-tagged $FOXO3^{WT}$, $FOXO3^{K259R}$, $FOXO3^{K271R}$, or $FOXO3^{K290}$. Whole-cell lysates (WCL) were immunoprecipitated with anti-EGFP and analyzed by immunoblotting with antibodies against the proteins shown on the right (Ac-K, acetyllysine). (B) Densitometric analysis of the immunoblotting results in (A) showing that SIRT3 deacetylates FOXO3 at K271 and K290, rather than K259. (C) Levels of FOXO3 acetylation in BAECs that were cotransfected with either scrambled siRNA or SIRT3 siRNA, together with EGFP-tagged $FOXO3^{K259R}$, $FOXO3^{K271R}$, or $FOXO3^{K290}$. WCL were immunoprecipitated with anti-EGFP and analyzed by immunoblotting with antibodies against the proteins shown on the right. (D) Densitometric analysis of the immunoblotting results in (C) showing that SIRT3 deacetylates FOXO3 at K271 and K290, rather than K259. All values are the mean ± SEM of the results from four independent experiments. Statistical analyses were performed by Student's *t* test between groups as indicated in the graphs. $^{*}p < 0.05$; $^{**}p < 0.01$.

hydrogen peroxide treatment. Although hydrogen peroxide treatment caused a small reduction in FOXO3 acetylation, levels of FOXO3 acetylation were significantly increased when SIRT3 was knocked down (Figs. 1C and D). These results suggest that hydrogen peroxide-induced SIRT3 deacetylates FOXO3.

SIRT3 deacetylates FOXO3 at K271 and K290

To characterize which lysine residue of FOXO3 is modulated by SIRT3, deacetylation mimetic lysine-to-arginine (KR) mutants [21] of FOXO3 were generated at K259, K271, and K290. K259 of FOXO3 is acetylated by p300/CBP, whereas K271 and K290 of FOXO3 are hypothesized to be targeted by SIRT1 [13]. In cells that overexpressed the dominant-negative mutant of SIRT3, SIRT3^{H248Y}, we observed enhancement of FOXO3 acetylation (Figs. 2A and B). When cells were transfected with SIRT3^{H248Y} together with the FOXO3^{K271R} or FOXO3^{K290R} mutants, the SIRT3^{H248Y}-driven enhancement of FOXO3 acetylation was abolished (Figs. 2A and B), but overexpression of SIRT3^{H248Y} still increased the level of FOXO3^{K259R} acetylation (Figs. 2A and B). The results were further assessed by cells cotransfected with SIRT3 siRNA together with various FOXO3 mutants. There was no increment in FOXO3 acetylation when the KR mutation was introduced at either K271 or K290 (Figs. 2C and D). In contrast, SIRT3 knockdown enhanced the level of FOXO3^{K259R} acetylation (Figs. 2C and D). All the data suggest that K271 and K290 rather than K259 of FOXO3 are targeted by SIRT3.

Deacetylation of FOXO3 promotes its nuclear localization

SIRT1-dependent deacetylation renders FOXO1 immobile within the nucleus, thereby promoting the transcription of FOXO1-dependent genes [22]. Nuclear localization of FOXO3 is essential for its transcriptional activity and is precisely controlled by multiple posttranslational modifications [13,15]. In this study, cells that overexpressed FOXO3$^{K271/290R}$ or FOXO3$^{K271/290Q}$ (acetylation mimetic mutant) were fractionated into nuclear, mitochondrial, and cytosolic components. We found that FOXO3$^{K271/290R}$ and FOXO3$^{K271/290Q}$ were present in all three subcellular compartments, but the two mutants exhibited distinct distributions. FOXO3$^{K271/290R}$ was preferentially localized in the nucleus compared with FOXO3$^{K271/290Q}$ ($33 \pm 6\%$ vs $14 \pm 2\%$; Figs. 3A and B). FOXO3$^{K271/290Q}$ showed a more prominent localization in the cytosol and mitochondria than did FOXO3$^{K271/290R}$ ($77 \pm 3\%$ vs $66 \pm 7\%$ in the cytosolic fraction; $9 \pm 3\%$ vs $1.6 \pm 0.4\%$ in the mitochondrial fraction; Figs. 3A and B). These results indicate that deacetylation of FOXO3 promotes its nuclear localization.

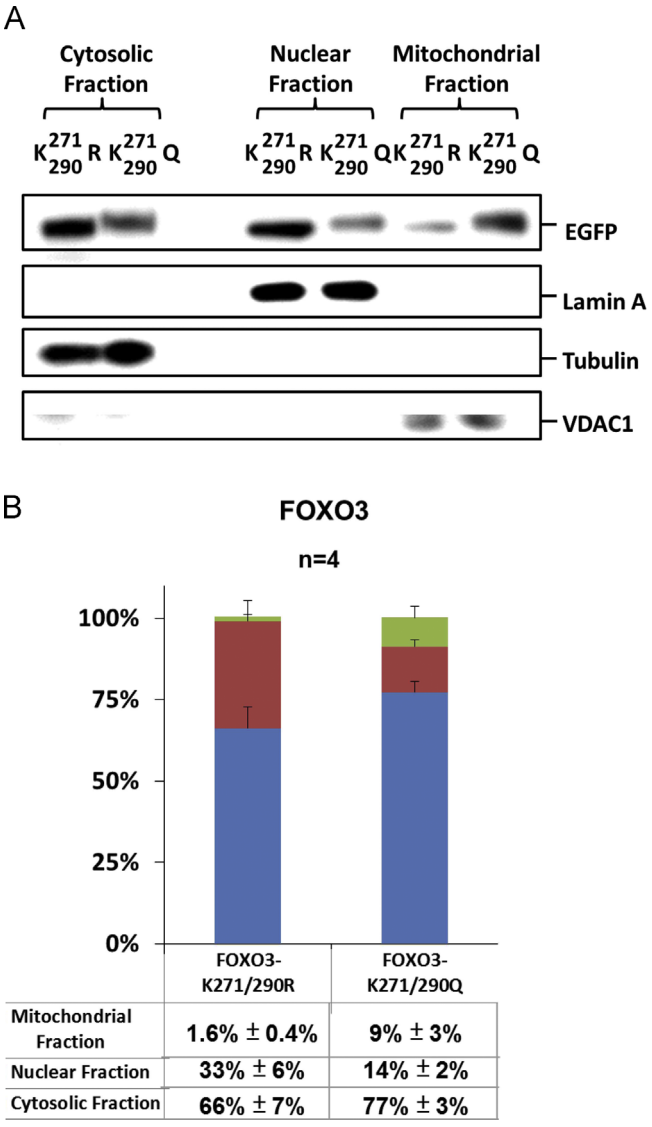

Fig. 3. Deacetylation of FOXO3 promotes its nuclear localization. (A) Fractionated cellular extracts (cytosolic, nuclear, and mitochondrial fractions) were prepared from BAECs that overexpressed FOXO3$^{K271/290R}$ or FOXO3$^{K271/290Q}$ and subjected to immunoblotting analysis. EGFP shows both FOXO3$^{K271/290R}$ and FOXO3$^{K271/290Q}$; tubulin shows cytosolic enrichment; lamin A shows nuclear enrichment; VDAC1 shows mitochondrial enrichment. (B) Densitometric analysis of the immunoblotting results showing the percentage of FOXO3$^{K271/290R}$ or FOXO3$^{K271/290Q}$ present in each of the three fractions.

SIRT3 deacetylates FOXO3 to regulate PGC-1α and TFAM

Increased expression of SIRT3 in adipocytes induces the expression of genes involved in mitochondrial biogenesis [23] and the maintenance of cellular ATP levels in heart, liver, and kidney [24]. PGC-1α, the master determinant of mitochondrial biogenesis, is transcriptionally regulated by FOXO3 [25]. When cells were treated with siRNA to SIRT3 or overexpressed SIRT3^{H248Y}, decreased levels of PGC-1α were detected (Figs. 4A and C). To investigate whether the expression of PGC-1α is regulated by SIRT3 through the deacetylation of FOXO3 at K271 and K290, cells were transfected with either SIRT3^{WT} or SIRT3^{H248Y} together with either the KR or the KQ mutant of FOXO3 [21]. We observed that SIRT3^{H248Y}-driven suppression of PGC-1α was restored in cells that overexpressed FOXO3$^{K271/290R}$, whereas the levels of PGC-1α were substantially reduced in cells that overexpressed the acetylation mimetic mutant, FOXO3$^{K271/290Q}$ (Figs. 4B and C). Consistent with this result, SIRT3–FOXO3 had a similar effect on TFAM, a downstream target of PGC-1α that is required for mitochondrial DNA replication and transcription [26] (Figs. 4A–C). These data suggest that SIRT3-mediated deacetylation of FOXO3 at K271 and K290 increases PGC-1α and TFAM expression.

SIRT3 deacetylates FOXO3 to promote mitochondrial biogenesis

We further observed that cells that overexpressed FOXO3$^{K271/290Q}$ had a 23% reduction in mitochondrial mass (Fig. 5A) and a 27% reduction in ATP levels compared with cells that overexpressed FOXO3$^{K271/290R}$ (Fig. 5B). Confocal microscopic analysis of MitoTracker-labeled cells showed that overexpression of SIRT3^{WT} induced extensive mitochondrial elongation, whereas overexpression of SIRT3^{H248Y} triggered mitochondrial fragmentation (Fig. 5C). Remarkably, overexpression of FOXO3$^{K271/290Q}$ abrogated SIRT3^{WT}-mediated mitochondrial elongation (Fig. 5C). Conversely, overexpression of FOXO3$^{K271/290R}$ reversed the SIRT3^{H248Y}-induced mitochondrial fragmentation and allowed normal mitochondrial elongation and interconnectedness (Fig. 5C). Fragmented mitochondria were found

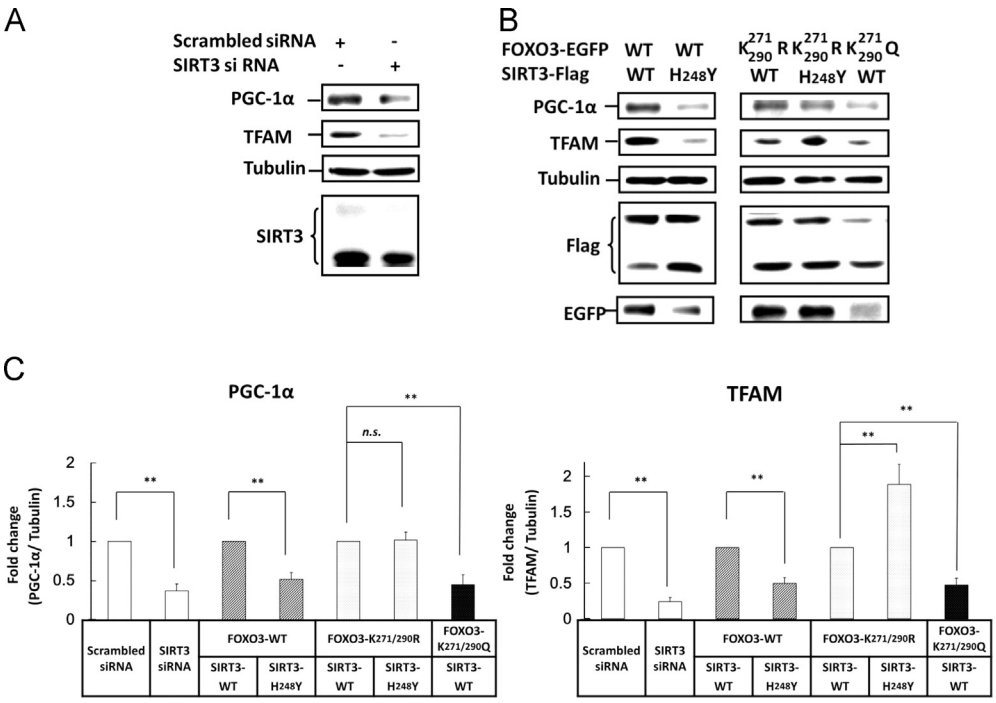

Fig. 4. SIRT3 deacetylates FOXO3 to regulate mediators of mitochondrial biogenesis. (A) Effects of SIRT3 on the expression of PGC-1α and TFAM. An immunoblot of extracts from HUVECs treated with a scrambled siRNA or SIRT3 siRNA is shown. (B) Effects of SIRT3-mediated deacetylation of FOXO3 on the expression of PGC-1α and TFAM. Immunoblots of extracts from BAECs that overexpress Flag-tagged $SIRT3^{WT}$ or $SIRT3^{H248Y}$, together with EGFP-tagged $FOXO3^{WT}$, $FOXO3^{K271/290R}$, or $FOXO3^{K271/290Q}$ are shown. (C) Densitometric analysis of the immunoblotting results in (A) and (B) showing that SIRT3 deacetylates FOXO3 at K271 and K290 to regulate expression levels of PGC-1α and TFAM. All values are the mean ± SEM of the results from five independent experiments. Statistical analyses were performed by Student's *t* test between groups as indicated in the graphs. $^{**}p < 0.01$; n.s., not significant.

in 75 of the 100 cells that overexpressed $SIRT3^{WT}$+$FOXO3^{K271/290Q}$; 20 had intermediate mitochondria and 5 had elongated mitochondria. Of the 100 cells that overexpressed $SIRT3^{H248Y}$+$FOXO3^{K271/290R}$, 23 had fragmented mitochondria, 29 had intermediate mitochondria, and 48 had elongated mitochondria. Taken together, these results indicate that SIRT3-mediated deacetylation of FOXO3 promotes mitochondrial biogenesis resulting in increased mitochondrial mass, ATP production, and interconnectedness.

SIRT3 deacetylates FOXO3 to regulate Drp1, Fis1, and Mfn2

The elongated mitochondrial phenotype that we observed in the cells that overexpressed $SIRT3^{WT}$ could result from defective mitochondrial fission as well as from upregulated mitochondrial biogenesis [2,27]. Thus, we analyzed whether SIRT3–FOXO3 regulates the expression of Drp1 and Fis1, essential mediators of mitochondrial fission [2,27,28], and of Mfn2, which is indispensable for mitochondrial fusion and is transcribed by PGC-1α [2]. Reduced levels of Drp1, Fis1, and Mfn2 were detected in cells transfected with SIRT3 siRNA or $SIRT3^{H248Y}$ relative to the controls (Figs. 6A, B, and C). Furthermore, $SIRT3^{H248Y}$-mediated suppression of Drp1, Fis1, and Mfn2 was overcome by overexpression of $FOXO3^{K271/290R}$ (Figs. 6B and C). In addition, overexpression of $FOXO3^{L\ K271/290Q}$ repressed Drp1, Fis1, and Mfn2, even in the presence of overexpressed $SIRT3^{WT}$ (Figs. 6B and C). These data indicate that SIRT3-mediated deacetylation of FOXO3 positively regulates Drp1, Fis1, and Mfn2 to coordinate mitochondrial fission and fusion. Therefore, the large interconnected mitochondrial morphology induced by SIRT3–FOXO3 (Fig. 5C) appears to result from mitochondrial biogenesis rather than from an imbalance in mitochondrial fission/fusion.

SIRT3 deacetylates FOXO3 to regulate Bnip3, Nix, and LC3

To maintain mitochondrial function and integrity, dysfunctional mitochondria must be detected and cleared by mitophagy, the selective autophagic degradation of mitochondria [2,29,30]. FOXO3 positively regulates the expression of the core mitophagic regulators Bnip3, Nix, and LC3 [31,32]. This prompted us to examine whether SIRT3-related deacetylation of FOXO3 affects mitophagy. When SIRT3 was knocked down in cells, levels of Nix, Bnip3, and LC3 were reduced relative to controls (Figs. 7A and C). Moreover, SIRT3 knockdown decreased the conversion of soluble LC3-I to lipid-bound LC3-II, which is a determining step for autophagosome formation (Figs. 7A and C) [33]. Consistent with this result, overexpression of $SIRT3^{H248Y}$ led to repression of all three mitophagic regulators (Figs. 7B and C). Overexpression of $FOXO3^{K271/290R}$ reversed the $SIRT3^{H248Y}$-mediated suppression of Nix, Bnip3, and LC3-II/LC3-I, whereas overexpression of $FOXO3^{K271/290Q}$ with $SIRT3^{WT}$ also reduced the expression of Nix, Bnip3, and LC3 (Figs. 7B and C). These data suggest that SIRT3 deacetylation of FOXO3 controls the primary mediators of mitophagy.

SIRT3 deacetylates FOXO3 to induce mitophagy in response to oxidative stress

p62 is implicated in the process of mitophagy. It recognizes polyubiquitinated mitochondrial substrates and mediates the sequestration of impaired mitochondria in the autophagosomes through its interaction with LC3. The trapped defective mitochondria are further degraded by lysosomal hydrolases in autolysosomes [34,35]. To establish whether deacetylation of FOXO3 at K271 and K290 mediates the elimination of damaged mitochondria, we examined whether p62 forms aggregates with ubiquitin

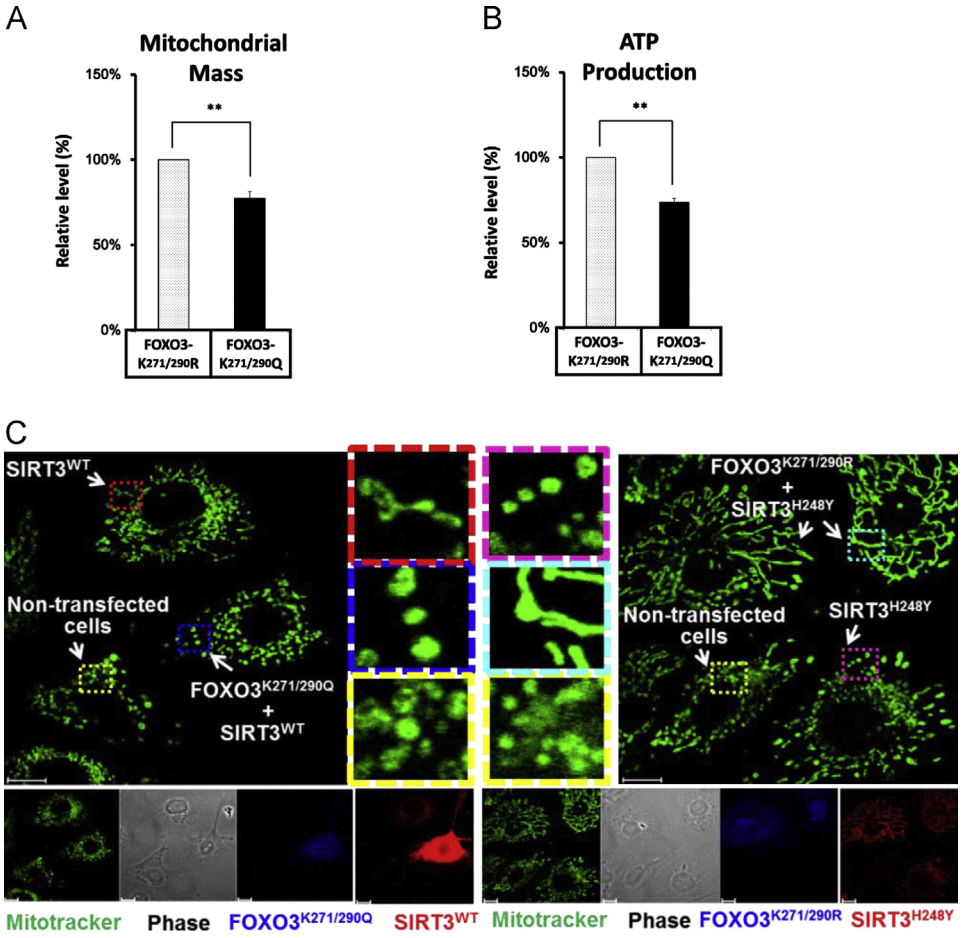

Fig. 5. SIRT3 deacetylates FOXO3 to promote mitochondrial biogenesis. (A) Effects of deacetylation of FOXO3 at K271 and K290 on mitochondrial mass. BAECs that overexpressed either FOXO3$^{K271/290R}$ or FOXO3$^{K271/290Q}$ were stained with MitoTracker, and their mitochondrial mass was measured by flow cytometry. Mitochondrial mass was expressed relative to that in the FOXO3$^{K271/290R}$ mutant. (B) Effects of deacetylation of FOXO3 at K271 and K290 on ATP production. Levels of ATP in BAECs that overexpressed either FOXO3$^{K271/290R}$ or FOXO3$^{K271/290Q}$ were measured with a bioluminescence cell assay kit. ATP level was expressed relative to that in the FOXO3$^{K271/290R}$ mutant. All values in (A) and (B) are the mean ± SEM of the results from six independent experiments. Statistical analyses were performed by Student's *t* test between groups as indicated in the graphs. $^{**}p < 0.01$. (C) Effects of SIRT3-mediated deacetylation of FOXO3 on mitochondrial networks. Representative confocal analysis of mitochondrial morphology in BAECs that overexpressed Flag-tagged SIRT3^{WT} or SIRT3^{H248Y} together with EGFP-tagged FOXO3^{WT}, FOXO3$^{K271/290R}$, or FOXO3$^{K271/290Q}$ (pseudo-colored blue) is shown. Cells were labeled with MitoTracker (pseudo-colored green) and then stained with antibodies against Flag-tagged SIRT3 (pseudo-colored red). Phase-contrast images depict endothelial cell morphology. The red dashed box contains a higher magnification image to show that SIRT3^{WT} promotes mitochondrial elongation. The image in the pink dashed box is at higher magnification to show that SIRT3^{H248Y} triggers mitochondrial fragmentation. The blue dashed box shows that FOXO3$^{K271/290Q}$ abrogates SIRT3^{WT}-mediated mitochondrial elongation. The light blue dashed box shows that FOXO3$^{K271/290R}$ overcomes SIRT3^{H248Y}-induced mitochondrial fragmentation. The yellow dashed boxes show normal mitochondrial morphology. Scale bars, 10 μm.

in the mitochondrial network. Cells that overexpressed EGFP-tagged FOXO3$^{K271/290R}$ or FOXO3$^{K271/290Q}$ along with HA-tagged ubiquitin and pDsRed2-Mito were treated with hydrogen peroxide (0.2 mM) for 14 h. Immunofluorescence of pDsRed2-Mito was used to show the mitochondrial network. Hydrogen peroxide stimulates the endogenous p62 to form aggregates with ubiquitin in both cells. However, the p62–ubiquitin aggregates were not colocalized with mitochondria in cells overexpressed that FOXO3$^{K271/290R}$, whereas the p62–ubiquitin aggregates did accumulate on mitochondria in cells that overexpressed FOXO3$^{K271/290Q}$ (Fig. 8A). The mitochondrial connectivity in cells that overexpressed FOXO3$^{K271/290R}$ appeared to be interrupted by the p62–ubiquitin aggregates (Fig. 8A), which possibly result from the degradation of mitochondria. We further assessed whether the mitochondrial clearance in cells that overexpressed FOXO3$^{K271/290R}$ occurs an autophagy-dependent manner. Cells that overexpressed the common autophagosome marker RFP-tagged LC3 along with EGFP-tagged FOXO3$^{K271/290R}$ or FOXO3$^{K271/290Q}$ were treated with hydrogen peroxide. Immunofluorescence of Lamp1 and Tom20 was used as a marker of lysosomes and mitochondria, respectively; colocalization of LC3 puncta and Lamp1 indicates the formation of autolysosomes [36]. Numerous and large LC3 puncta were detected in close proximity to mitochondria in cells that overexpressed FOXO3$^{K271/290R}$ but not in cells that overexpressed FOXO3$^{K271/290Q}$ (Fig. 8B). Moreover, the large LC3 puncta, detected in the cells that overexpressed FOXO3$^{K271/290R}$, were predominantly colocalized with Lamp1 but not Tom20 (Fig. 8B). The mitochondrial connectivity in cells overexpressing FOXO3$^{K271/290R}$ also appeared to be interrupted by the autolysosomes, as evidenced by the occurrence of mitophagy at these sites (Fig. 8B). Strikingly, the colocalization of LC3 puncta and Lamp1 was rarely detected in cells that overexpressed FOXO3$^{K271/290Q}$ (Fig. 8B). Of the 100 cells that overexpressed FOXO3$^{K271/290R}$, 69 were mitochondrial autolysosome positive; of the 100 cells that overexpressed FOXO3$^{K271/290Q}$, 5 were mitochondrial autolysosome positive. In addition, we observed that mitochondria in cells that overexpressed FOXO3$^{K271/290R}$ detected by either overexpression of pDsRed2-Mito or immunostaining with antibodies against Tom20 exhibited long and interconnected morphology under oxidative stress (Figs. 8A and B). In contrast, the mitochondria in cells that overexpressed FOXO3$^{K271/290Q}$ were damaged by hydrogen peroxide to become fragmented (Figs. 8A and B). All these

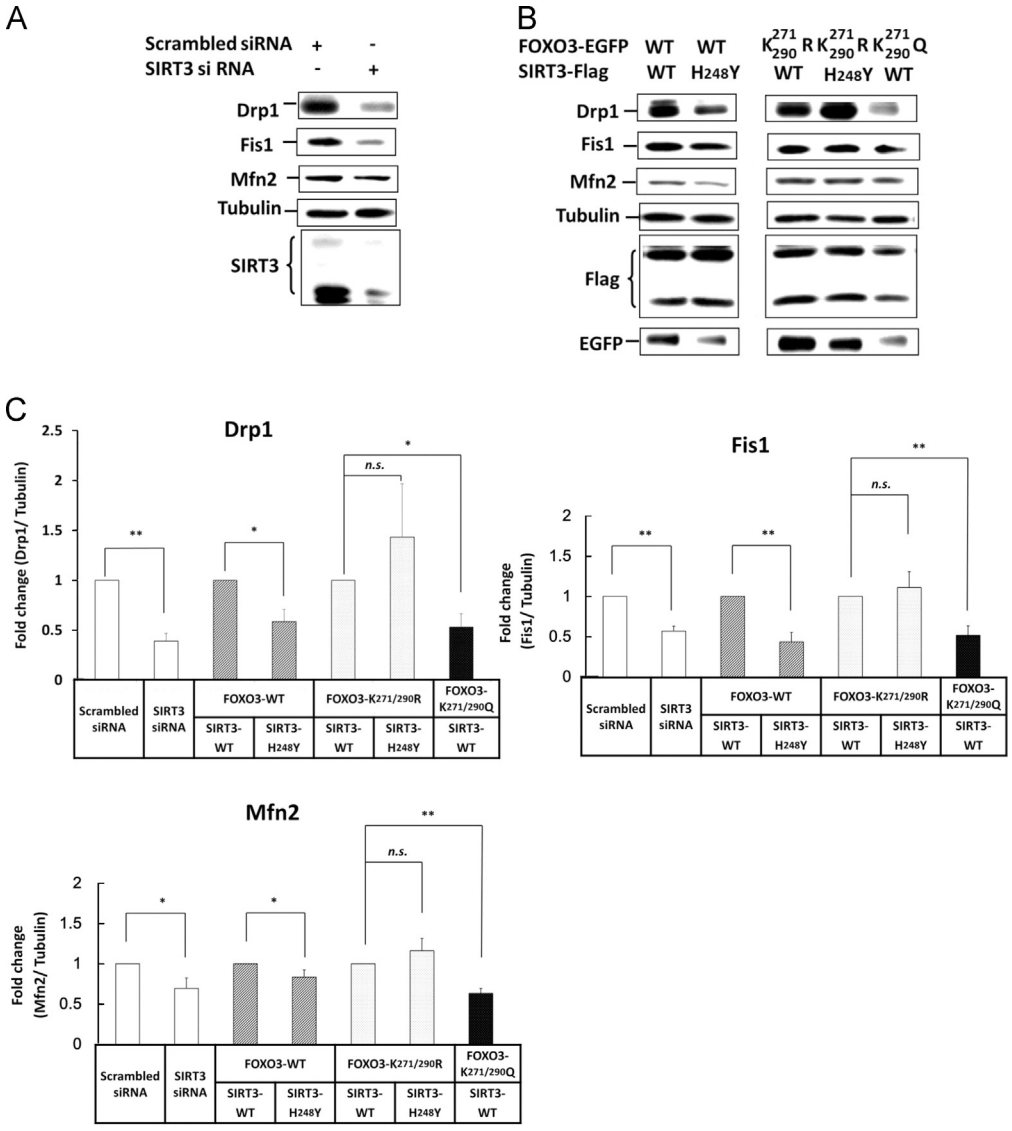

Fig. 6. SIRT3 deacetylates FOXO3 to regulate mediators of mitochondrial fission and fusion. (A) Effects of SIRT3 on expression of Drp1, Fis1, and Mfn2. Immunoblots of extracts from HUVECs that were treated with a scrambled siRNA or SIRT3 siRNA are shown. (B) Effects of SIRT3-mediated deacetylation of FOXO3 on the expression of Drp1, Fis1, and Mfn2. Immunoblots of extracts from BAECs that overexpressed Flag-tagged $SIRT3^{WT}$ or $SIRT3^{H248Y}$ together with EGFP-tagged $FOXO3^{WT}$, $FOXO3^{K271/290R}$, or $FOXO3^{K271/290Q}$ are shown. (C) Densitometric analysis of the immunoblotting results in (A) and (B) showing that SIRT3 deacetylates FOXO3 at K271 and K290 to regulate the expression of Drp1, Fis1, and Mfn2. All values are the mean ± SEM of the results from five independent experiments. Statistical analyses were performed by Student's *t* test between groups as indicated in the graphs. $^{*}p < 0.05$; $^{**}p < 0.01$; n.s., not significant.

results indicate that SIRT3-mediated deacetylation of FOXO3 at K271 and K290 induces the mitophagic system to eliminate ROS-damaged mitochondria and protect cells against oxidative stress.

SIRT3 deacetylates FOXO3 to preserve mitochondrial bioenergetic reserve capacity in response to oxidative stress

To examine whether SIRT3-mediated deacetylation of FOXO3 at K271 and K290 protects mitochondrial function against oxidative stress, cells were cotransfected with SIRT3 siRNA and the $FOXO3^{K271/290R}$, $FOXO3^{K271/290Q}$, or $FOXO3^{K259R}$ overexpression plasmid. These cells were challenged with hydrogen peroxide (0.2 mM) for 14 h, and their respiratory profiles were then assessed. Hydrogen peroxide-exposed cells exhibited a significant reduction in basal respiration, maximum respiration, ATP-coupled respiration, and spare capacity compared with the untreated cells (Figs. 9A–D). When cells that were depleted of SIRT3 were treated with hydrogen peroxide, a small but significant reduction in basal respiration occurred (Fig. 9A), and there were significant decreases in maximum respiration, ATP-coupled respiration, and spare capacity compared with scrambled siRNA-transfected control cells (Figs. 9B–D). The SIRT3 siRNA-driven reduction in mitochondrial respiration was restored by overexpression of $FOXO3^{K271/290R}$, but not by overexpression of $FOXO3^{K271/290Q}$ or $FOXO3^{K259R}$. Our results demonstrate that SIRT3 plays a minor role in the control of basal respiration in mitochondria, which is consistent with previous findings [37]. However, SIRT3 has dominant positive effects on the maximum respiration, ATP-coupled respiration, and spare capacity of mitochondria via deacetylation of FOXO3 at K271 and K290. The results also confirm that hydrogen peroxide decreases the bioenergetics of intact cells and suggest that SIRT3-mediated deacetylation of FOXO3 at K271 and K290 is important for maintaining mitochondrial reserve capacity to protect cells against oxidative stress.

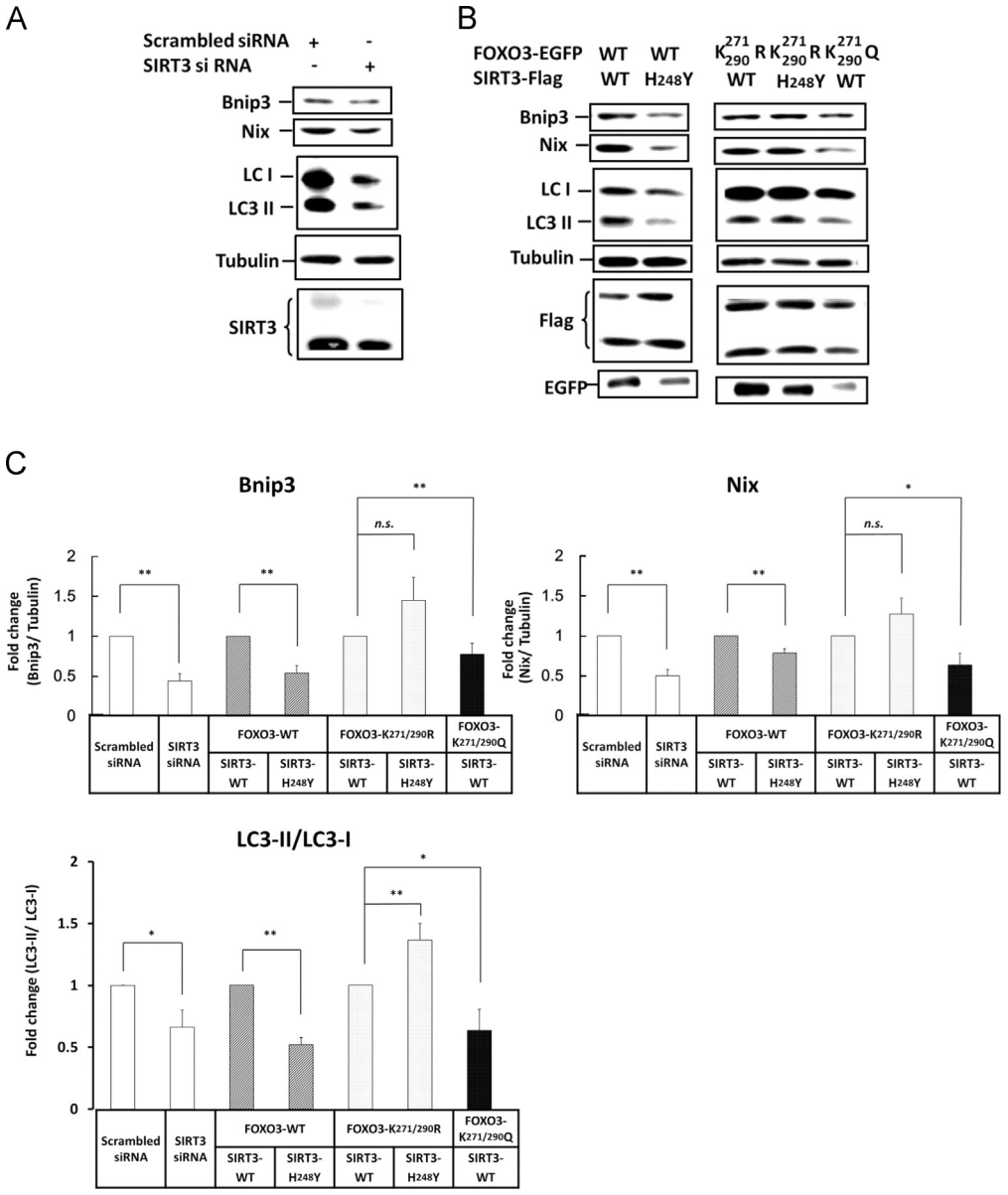

Fig. 7. SIRT3 deacetylates FOXO3 to regulate mediators of mitophagy. (A) Effects of SIRT3 on expression of Bnip3, Nix, and LC3-II/LC3-I. Immunoblots of extracts from HUVECs that were treated with a scrambled siRNA or SIRT3 siRNA are shown. (B) Effects of SIRT3-mediated deacetylation of FOXO3 on the expression of Bnip3, Nix, and LC3-II/LC3-I. Immunoblots of extracts from BAECs that overexpressed Flag-tagged $SIRT3^{WT}$ or $SIRT3^{H248Y}$ together with EGFP-tagged $FOXO3^{WT}$, $FOXO3^{K271/290R}$, or $FOXO3^{K271/290Q}$ are shown. (C) Densitometric analysis of the immunoblotting results in (A) and (B) showing that SIRT3 deacetylates FOXO3 at K271 and K290 to regulate the expression of Bnip3, Nix, and LC3-II/LC3-I. All values are the mean ± SEM of the results from five independent experiments. Statistical analyses were performed by Student's *t* test between groups as indicated in the graphs. $^{*}p < 0.05$; $^{**}p < 0.01$; n.s., not significant.

Discussion

Mitochondria are central for cellular metabolism, energy homeostasis, the stress response, and cell death. Defective mitochondria accumulate in cells during aging [1,2]. The functional and structural maintenance of mitochondria depends on the proper balance between mitochondrial biogenesis and mitophagy, which is assisted by mitochondrial fusion/fission [2].

The capacity for mitochondrial biogenesis decreases with increasing age [2,38]. CR-induced SIRT1 promotes mitochondrial biogenesis via increases in PGC-1α, NRF-1, and TFAM [39,40]. Our results demonstrate that SIRT3-mediated deacetylation of FOXO3 upregulates the expression of PGC-1α and TFAM to control mitochondrial mass and ATP production in cells. In addition, the deacetylation of FOXO3 by SIRT3 leads to the elongation of and greater interconnectedness between mitochondria, which potentially could result from a reduction in mitochondrial fission. However, the main mediators of mitochondrial fission, Drp1 and Fis1, are positively regulated by SIRT3–FOXO3, as is the PGC-1α-controlled mitochondrial fusion protein Mfn2. Therefore, the mitochondrial morphologic changes elicited by SIRT3–FOXO3 should result from the increase in mitochondrial number, not from the declines in mitochondrial fission. Moreover, the activity of Drp1, Fis1, and Mfn2 can assist the distribution and division of the newly formed mitochondria. The deacetylation of FOXO3 by SIRT3 may play a supporting role in energy production for cellular viability and vitality via mitochondrial biogenesis.

A progressive decline in autophagosomal degradation of cellular proteins or organelles has been proposed as a primary cause of aging [41]. SIRT1 deacetylates FOXO3 to attenuate hypoxia-associated mitochondrial and renal damage via Bnip3-dependent autophagy in response to CR [32]. Our data demonstrate that the

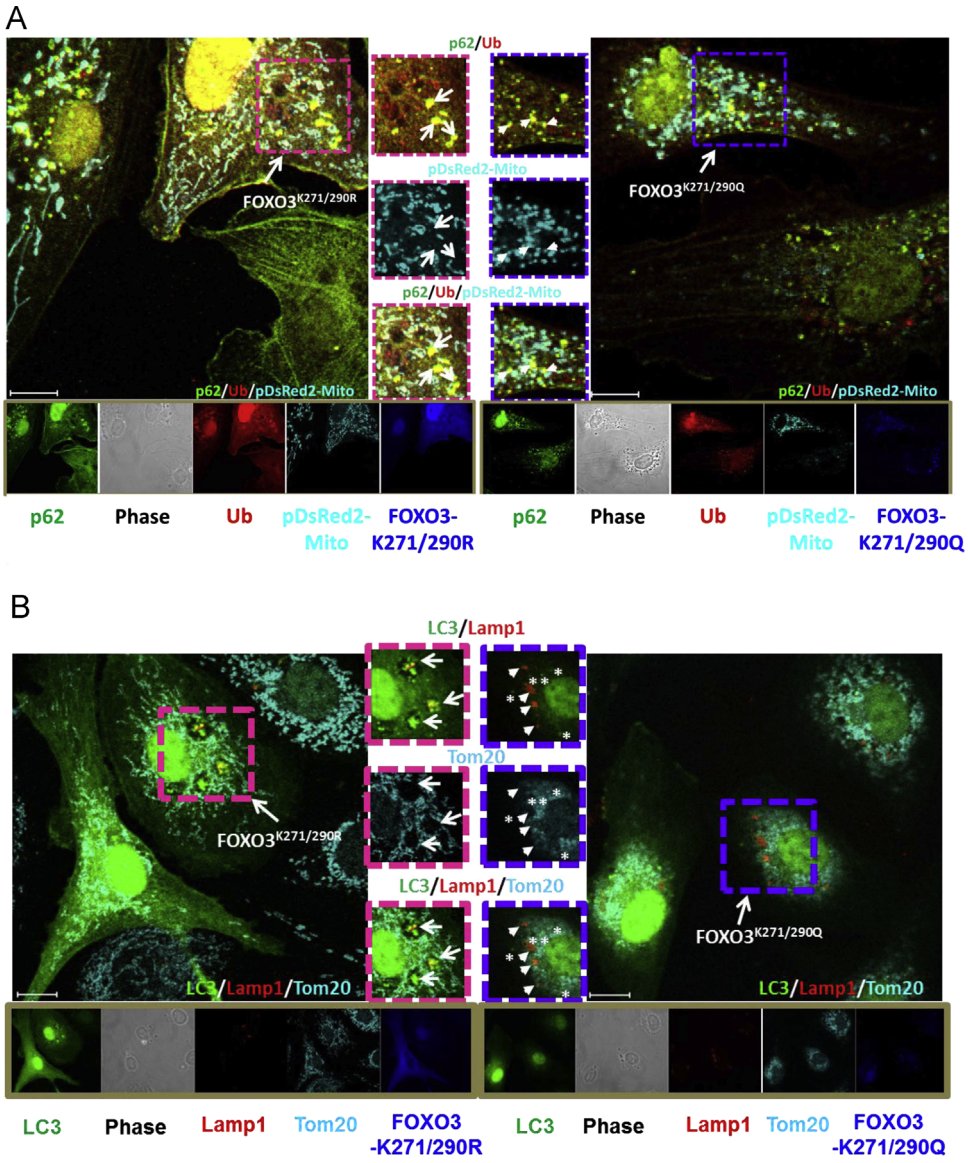

Fig. 8. SIRT3 deacetylates FOXO3 to induce mitophagy in response to oxidative stress. (A) Effects of the deacetylation of FOXO3 at K271 and K290 on p62 aggregation in cells under oxidative stress. Representative confocal analysis of p62 in BAECs that overexpressed EGFP-tagged FOXO3$^{K271/290R}$ or FOXO3$^{K271/290Q}$ (pseudo-colored blue) together with HA-tagged ubiquitin (pseudo-colored red) and pDsRed2-Mito (pseudo-colored cyan) is shown. Cells were treated with hydrogen peroxide (0.2 mM) for 14 h and then were processed for immunostaining with antibodies against p62 (pseudo-colored green). Phase-contrast images depict EC morphology. Hydrogen peroxide induced p62 aggregation (green) to colocalize with ubiquitin (Ub; red) and mitochondria (cyan) in cells that overexpressed FOXO3$^{K271/290Q}$, whereas the p62–ubiquitin aggregates (yellow) were not colocalized with mitochondria (cyan) in cells that overexpressed FOXO3$^{K271/290R}$. Pink dashed boxes show the region containing detectable p62–ubiquitin aggregates (arrows) located in close proximity to mitochondria in cells that overexpressed FOXO3$^{K271/290R}$. Purple dashed boxes show the region having accumulation of p62–ubiquitin aggregates (arrowheads) on mitochondria in cells that overexpressed FOXO3$^{K271/290Q}$. Scale bars, 10 μm. (B) Effects of deacetylation of FOXO3 at K271 and K290 on mitophagy in response to oxidative stress. Representative confocal analysis of mitophagy in BAECs that overexpressed RFP-tagged LC3 (pseudo-colored green) together with EGFP-tagged FOXO3$^{K271/290R}$ or FOXO3$^{K271/290Q}$ (pseudo-colored blue) is shown. Cells were treated with hydrogen peroxide (0.2 mM) for 14 h and then were processed for immunostaining with antibodies against the lysosomal marker Lamp1 (pseudo-colored red) and the mitochondrial marker Tom20 (pseudo-colored cyan). Phase-contrast images depict EC morphology. Hydrogen peroxide induced autophagosomes (LC3 puncta, green) to fuse with lysosomes (Lamp1 puncta, red) and consequently form autolysosomes (yellow) in cells that overexpressed FOXO3$^{K271/290R}$, whereas there were no detectable autolysosomes in cells that overexpressed FOXO3$^{K271/290Q}$. Pink dashed boxes show the region containing detectable autolysosomes (arrows) located in close proximity to mitochondria in cells that overexpressed FOXO3$^{K271/290R}$. Purple dashed boxes show the region having detectable LC3 puncta (asterisks) and lysosomes (arrowheads) in close proximity to mitochondria in cells that overexpressed FOXO3$^{K271/290Q}$. Scale bars, 10 μm.

main mitophagic mediators, Bnip3, Nix, and LC3, are positively controlled by SIRT3 through deacetylation of FOXO3. In particular, when cells were challenged by hydrogen peroxide, the deacetylation mimetic mutant FOXO3$^{K271/290R}$ allowed the p62 clustering of ubiquitinated substrates and the formation of autolysosomes in proximity to mitochondria. However, there was no obvious existence of autolysosomes in cells that overexpressed the acetylation mimetic mutant FOXO3$^{K271/290Q}$, even when the p62 aggregates anchored on mitochondria. Mitophagy seems to be induced only in cells that overexpress FOXO3$^{K271/290R}$. Excessive accumulation of p62 clustering of ubiquitinated substrates triggers cell death in the absence of its degradation by autophagy [34,35]. The defect in removal of p62 clustering mitochondria by mitophagy may be deleterious to cells that overexpress FOXO3$^{K271/290Q}$. Mitochondrial quality is also secured through the mitochondrial fission and fusion [2,27,28]. The induction of Mfn2 by SIRT3–FOXO3 could promote mitochondrial fusion to mediate repair of damaged mitochondrial DNA [27,28], whereas the enhancement of Drp1

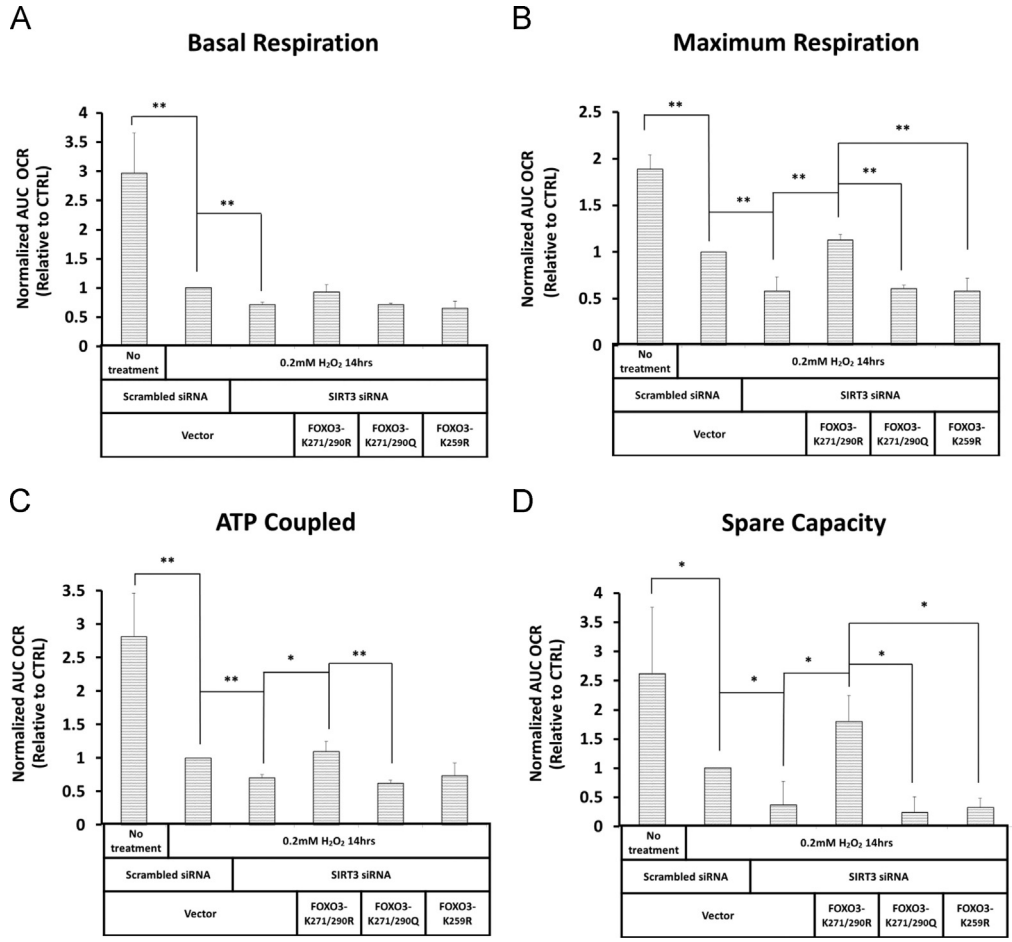

Fig. 9. SIRT3 deacetylates FOXO3 to preserve mitochondrial respiration capacity in response to oxidative stress. The effects of SIRT3-mediated deacetylation of FOXO3 on oxygen consumption rate (OCR) in response to hydrogen peroxide are shown. BAECs that were cotransfected with the indicated siRNA and DNA plasmid were treated with hydrogen peroxide (0.2 mM) for 14 h before measurement of OCR characteristics as follows: (A) basal respiration; (B) maximal respiration; (C) ATP-coupled respiration; and (D) spare capacity. All OCR values were recorded, and the AUC values were calculated before and after each drug injection. The relative AUC OCR values are expressed as the fold change in the hydrogen peroxide-treated cells cotransfected with SIRT3 siRNA and either a FOXO3 vector or a FOXO3 mutant with respect to those transfected with the control scrambled siRNA and a control vector.

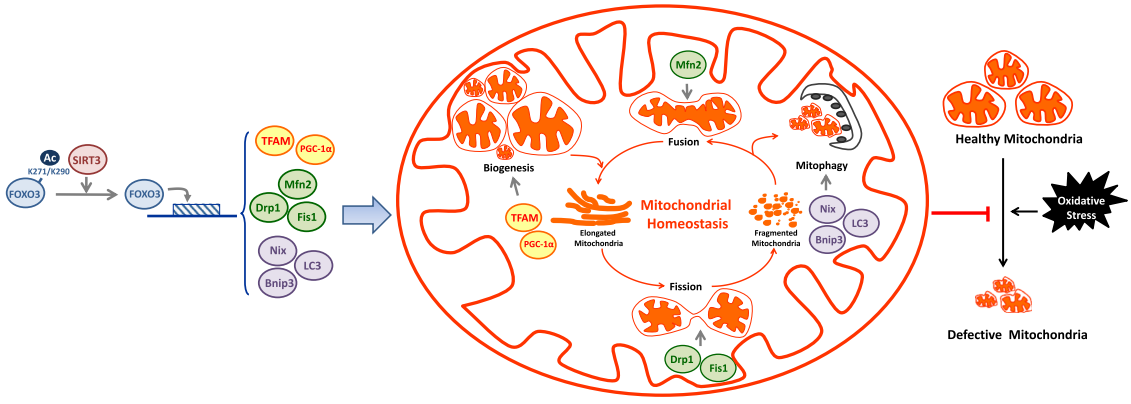

Fig. 10. Scheme illustrating SIRT3 deacetylates FOXO3 at K271 and K290 to protect mitochondria against oxidative stress by enhancing mitochondrial homeostasis.

and Fis1 could trigger the isolation of damaged mitochondria from healthy mitochondria so that they can be targeted for degradation [27,28]. On the basis of our findings, we suggest that SIRT3 ensures mitochondrial quality via deacetylation of FOXO3.

Increased oxidative stress causes endothelial dysfunction by reducing mitochondrial ATP production and disturbing mitochondrial redox balance, thereby enhancing the risk of developing cardiovascular diseases [42]. The profile of how SIRT3-mediated deacetylation of FOXO3 regulates mitochondrial bioenergetic function in response to oxidative stress was unraveled by extracellular flux analyses in our study. The hydrogen peroxide-decreased mitochondrial respiration is exacerbated by knockdown of SIRT3, but the effects of this are reversed by overexpression of FOXO3$^{K271/290R}$. These findings suggest that the hydrogen peroxide-induced SIRT3 elicits an adaptive response to prevent mitochondrial energy collapse via deacetylation of FOXO3 at K271 and K290.

Mouse SIRT3 can interact with FOXO3 in the nucleus and in mitochondria [7,16]. Recently, human SIRT3 was found to bind to chromatin in the nucleus and regulate stress-related genes through its histone deacetylase activity [43]. More than 98% of the total protein complement of mitochondria is nuclear-encoded, translated in the cytosol, and imported into the mitochondria [2,38]. Our data demonstrate that $FOXO3^{K271/290R}$ is preferentially localized in the nucleus in contrast to $FOXO3^{K271/290Q}$. All of the downstream targets of FOXO3 investigated in this study are nuclear-encoded mitochondrial proteins, involved in mitochondrial biogenesis, mitophagy, and mitochondrial fission/fusion. These findings raise the possibility that SIRT3 deacetylates FOXO3 in the nucleus to build the nucleus-to-mitochondria communication for diverse regulations of mitochondria. The retrograde communication can also be achieved by SIRT3–FOXO3 in the nucleus. In response to oxidative damage, SIRT3–FOXO3 maintains mitochondrial bioenergetic function to preserve ATP, which may provide fuels for DNA replication and DNA repair. Mitochondrial ROS can be reduced by SIRT3–FOXO3 through an increase in manganese superoxide dismutase and catalase [7] or through the upregulation of PGC-1α to interact with FOXO3 for transcriptional activation of a set of mitochondrial antioxidant enzymes [44]. Consequently, the oxidative damage to nuclear DNA is suppressed and the nuclear redox signaling is affected, the effects of which enhance cellular tolerance to oxidative damage [45]. However, it is also possible that SIRT3 deacetylates FOXO3 in the mitochondria to initiate an indirect signaling pathway that activates gene expression in the nucleus. We also cannot exclude the possibility that the deacetylation of FOXO3 by SIRT3 promotes the translocation of FOXO3 from mitochondria to nucleus, resulting in a complex influence on the transcription of nuclear genes controlling mitochondria.

Damage to the endothelium contributes to the function and metastasis of cancer cells, to tumor growth, and to the development of cardiovascular disease. Healthy ECs inhibit cancer cell invasiveness, proliferation, and inflammatory signaling [46]. SIRT3 protects against carcinogenesis by maintaining mitochondrial integrity and metabolism during oxidative stress [8]. FOXO3 acts as a tumor suppressor by upregulating genes involved in stress resistance, metabolism, cell cycle arrest, and apoptosis [13,15]. Our results with cultured ECs show that SIRT3-mediated deacetylation of FOXO3 increases cellular resistance to oxidative stress by enhancing mitochondrial homeostasis, which provides an addition clue to how SIRT3 and FOXO3 play their roles in tumor suppression.

Endothelial dysfunction can result from and/or contribute to the pathogenesis of obesity and diabetes [47]. The reduction in mitochondrial biogenesis, defects in energy production, and accumulation of mitochondrial ROS are risk factors causing insulin resistance in the development of obesity and diabetes [48]. High-fat diet feeding in mice leads to a significantly elevated ROS accumulation, reduced mitochondrial density, downregulation of PGC-1α and TFAM, increased mitochondrial dysfunction, and increment in FOXO3 phosphorylation [49]. On the other hand, reduced activity of SIRT3 and increased mitochondrial protein oxidation are detected in mice chronically fed a high-fat diet [50]. PGC-1α regulates mitochondrial biogenesis that is critical to the maintenance of energy metabolism, mitochondrial content, and function. Mice display insulin resistance when PGC-1α is knocked out in adipose tissues [51]. However, increased mitochondrial biogenesis is accompanied by the generation of ROS, which interferes with the insulin signaling pathway and leads to the progression of insulin resistance [48]. A recent report shows that the systemic removal of hydrogen peroxide by PEGylated catalase in obese mice effectively improves insulin resistance [52]. Multiple mitochondrial antioxidant enzymes are transcriptionally regulated by the interaction between SIRT3 and FOXO3 [7] or by the interaction between PGC-1α and FOXO3 [44]. Hence, SIRT3–FOXO3 may improve insulin resistance by enhancing mitochondrial biogenesis and the mitochondrial ROS-detoxifying system, thereby mitigating the onset and progression of diabetes and obesity.

In summary, our results demonstrate that oxidative stress induces SIRT3 to deacetylate FOXO3 at K271 and K290, further enhancing mitochondrial homeostasis via the coordination of mitochondrial biogenesis, fission/fusion, and mitophagy. The resulting improvement in mitochondrial quantity and quality maintains the mitochondrial reserve capacity to protect cells against oxidative stress (Fig. 10). Maladaptation to oxidative stress is a root cause of aging and various diseases . Our findings provide new strategies for improving cellular adaptation to stress, providing a promising direction for aging-delaying and disease intervention therapies.

Acknowledgments

This work was supported by grants from the Academia Sinica and the National Science Council of Taiwan (NSC99-2320-B-001-010-MY3). We thank Kerry Ko for manuscript editing. We also thank Dr. Wei-Chien Huang (China Medical University, Taiwan) for the FOXO3 constructs, Dr. Chun-Hua Hsu (National Taiwan University) for the SIRT3 cDNA, Dr. Hsiu-Ming Shih (Academia Sinica, Taiwan) for the human ubiquitin–HA expression plasmid, and Dr. Guang-Chao Chen (Academia Sinica) for the pmRFP-LC3 expression plasmid. We also acknowledge Kuan-Yu Chou (Academia Sinica) and Show-Rong Ma (Academia Sinica) for helpful instruction on confocal microscopy and Chia-Hao Chou (Cell-Bio Co., Ltd.) for helpful instruction on the Seahorse XF-24 bioanalyzer.

References

[1] Guarente, L. Mitochondria—a nexus for aging, calorie restriction, and sirtuins? *Cell* **132:**171–176; 2008.
[2] Seo, A. Y.; Joseph, A. M.; Dutta, D.; Hwang, J. C. Y.; Aris, J. P.; Leeuwenburgh, C. New insights into the role of mitochondria in aging: mitochondrial dynamics and more. *J. Cell Sci.* **123:**2533–2542; 2010.
[3] Yen, W. L.; Klionsky, D. J. How to live long and prosper: autophagy, mitochondria, and aging. *Physiology* **23:**248–262; 2008.
[4] Donmez, G.; Guarente, L. Aging and disease: connections to sirtuins. *Aging Cell* **9:**285–290; 2010.
[5] Guarente, L.; Picard, F. Calorie restriction—the SIR2 connection. *Cell* **120:**473–482; 2005.
[6] Finkel, T.; Deng, C. -X.; Mostoslavsky, R. Recent progress in the biology and physiology of sirtuins. *Nature* **460:**587–591; 2009.
[7] Sundaresan, N. R.; Gupta, M.; Kim, G.; Rajamohan, S. B.; Isbatan, A.; Gupta, M. P. Sirt3 blocks the cardiac hypertrophic response by augmenting Foxo3a-dependent antioxidant defense mechanisms in mice. *J. Clin. Invest.* **119:**2758–2771; 2009.
[8] Kim, H. -S.; Patel, K.; Muldoon-Jacobs, K.; Bisht, K. S.; Aykin-Burns, N.; Pennington, J. D.; van der Meer, R.; Nguyen, P.; Savage, J.; Owens, K. M. SIRT3 is a mitochondria-localized tumor suppressor required for maintenance of mitochondrial integrity and metabolism during stress. *Cancer Cell* **17:**41–52; 2010.
[9] Qiu, X.; Brown, K.; Hirschey, M. D.; Verdin, E.; Chen, D. Calorie restriction reduces oxidative stress by SIRT3-mediated SOD2 activation. *Cell Metab.* **12:**662–667; 2010.
[10] Someya, S.; Yu, W.; Hallows, W. C.; Xu, J.; Vann, J. M.; Leeuwenburgh, C.; Tanokura, M.; Denu, J. M.; Prolla, T. A. Sirt3 mediates reduction of oxidative damage and prevention of age-related hearing loss under caloric restriction. *Cell* **143:**802–812; 2010.
[11] Hirschey, M. D.; Shimazu, T.; Goetzman, E.; Jing, E.; Schwer, B.; Lombard, D. B.; Grueter, C. A.; Harris, C.; Biddinger, S.; Ilkayeva, O. R.; Stevens, R. D.; Li, Y.; Saha, A. K.; Ruderman, N. B.; Bain, J. R.; Newgard, C. B.; Farese Jr R. V.; Alt, F. W.; Kahn, C. R.; Verdin, E. SIRT3 regulates mitochondrial fatty-acid oxidation by reversible enzyme deacetylation. *Nature* **464:**121–125; 2010.
[12] Sundaresan, N. R.; Samant, S. A.; Pillai, V. B.; Rajamohan, S. B.; Gupta, M. P. SIRT3 is a stress-responsive deacetylase in cardiomyocytes that protects cells from stress-mediated cell death by deacetylation of Ku70. *Mol. Cell. Biol.* **28:**6384–6401; 2008.
[13] Calnan, D. R.; Brunet, A. The FoxO code. *Oncogene* **27:**2276–2288; 2008.
[14] van der Horst, A.; Burgering, B. M. T. Stressing the role of FoxO proteins in lifespan and disease. *Nat. Rev. Mol. Cell Biol.* **8:**440–450; 2007.
[15] Vogt, P. K.; Jiang, H.; Aoki, M. Triple layer control: phosphorylation, acetylation and ubiquitination of FOXO proteins. *Cell Cycle* **4:**908–913; 2005.
[16] Jacobs, K. M.; Pennington, J. D.; Bisht, K. S.; Aykin-Burns, N.; Kim, H. S.; Mishra, M.; Sun, L.; Nguyen, P.; Ahn, B. H.; Leclerc, J.; Deng, C. X.; Spitz, D. R.; Gius, D. SIRT3

interacts with the daf-16 homolog FOXO3a in the mitochondria, as well as increases FOXO3a dependent gene expression. *Int. J. Biol. Sci.* **4:**291–299; 2008.
[17] Green, D. R.; Galluzzi, L.; Kroemer, G. Mitochondria and the autophagy–inflammation–cell death axis in organismal aging. *Science* **333:**1109–1112; 2011.
[18] Frossi, B.; Tell, G.; Spessotto, P.; Colombatti, A.; Vitale, G.; Pucillo, C. H_2O_2 induces translocation of APE/Ref-1 to mitochondria in the Raji B-cell line. *J. Cell. Physiol.* **193:**180–186; 2002.
[19] Mai, S.; Klinkenberg, M.; Auburger, G.; Bereiter-Hahn, J.; Jendrach, M. Decreased expression of Drp1 and Fis1 mediates mitochondrial elongation in senescent cells and enhances resistance to oxidative stress through PINK1. *J. Cell Sci* **123:**917–926; 2010.
[20] Terman, A.; Kurz, T.; Navratil, M.; Arriaga, E. A.; Brunk, U. T. Mitochondrial turnover and aging of long-lived postmitotic cells: the mitochondrial–lysosomal axis theory of aging. *Antioxid. Redox Signaling* **12:**503–535; 2010.
[21] Matsuzaki, H.; Daitoku, H.; Hatta, M.; Aoyama, H.; Yoshimochi, K.; Fukamizu, A. Acetylation of Foxo1 alters its DNA-binding ability and sensitivity to phosphorylation. *Proc. Natl. Acad. Sci. USA* **102:**11278–11283; 2005.
[22] Frescas, D.; Valenti, L.; Accili, D. Nuclear trapping of the forkhead transcription factor FoxO1 via Sirt-dependent deacetylation promotes expression of glucogenetic genes. *J. Biol. Chem* **280:**20589–20595; 2005.
[23] Shi, T.; Wang, F.; Stieren, E.; Tong, Q. SIRT3, a mitochondrial sirtuin deacetylase, regulates mitochondrial function and thermogenesis in brown adipocytes. *J. Biol. Chem.* **280:**13560–13567; 2005.
[24] Ahn, B. H.; Kim, H. S.; Song, S.; Lee, I. H.; Liu, J.; Vassilopoulos, A.; Deng, C. X.; Finkel, T. A role for the mitochondrial deacetylase Sirt3 in regulating energy homeostasis. *Proc. Natl. Acad. Sci. USA* **105:**14447–14452; 2008.
[25] Borniquel, S.; Garcia-Quintans, N.; Valle, I.; Olmos, Y.; Wild, B.; Martinez-Granero, F.; Soria, E.; Lamas, S.; Monsalve, M. Inactivation of Foxo3a and subsequent downregulation of PGC-1 mediate nitric oxide-induced endothelial cell migration. *Mol. Cell. Biol.* **30:**4035–4044; 2010.
[26] Ryan, M. T.; Hoogenraad, N. J. Mitochondrial–nuclear communications. *Annu. Rev. Biochem.* **76:**701–722; 2007.
[27] Liesa, M.; Palacin, M.; Zorzano, A. Mitochondrial dynamics in mammalian health and disease. *Physiol. Rev.* **89:**799–845; 2009.
[28] Chen, H.; Chan, D. C. Mitochondrial dynamics—fusion, fission, movement, and mitophagy—in neurodegenerative diseases. *Hum. Mol. Genet* **18:**R169–176; 2009.
[29] Zhang, J.; Ney, P. A. Role of BNIP3 and NIX in cell death, autophagy, and mitophagy. *Cell Death Differ.* **16:**939–946; 2009.
[30] Zhang, J.; Ney, P. A. Mechanisms and biology of B-cell leukemia/lymphoma 2/adenovirus E1B interacting protein 3 and Nip-like protein X. *Antioxid. Redox Signaling* **14:**1959–1969; 2011.
[31] Real, P. J.; Benito, A.; Cuevas, J.; Berciano, M. T.; de Juan, A.; Coffer, P.; Gomez-Roman, J.; Lafarga, M.; Lopez-Vega, J. M.; Fernandez-Luna, J. L. Blockade of epidermal growth factor receptors chemosensitizes breast cancer cells through up-regulation of Bnip3L. *Cancer Res.* **65:**8151–8157; 2005.
[32] Kume, S.; Uzu, T.; Horiike, K.; Chin-Kanasaki, M.; Isshiki, K.; Araki, S.; Sugimoto, T.; Haneda, M.; Kashiwagi, A.; Koya, D. Calorie restriction enhances cell adaptation to hypoxia through Sirt1-dependent mitochondrial autophagy in mouse aged kidney. *J. Clin. Invest.* **120:**1043–1055; 2010.
[33] Kimura, S.; Fujita, N.; Noda, T.; Yoshimori, T. Monitoring autophagy in mammalian cultured cells through the dynamics of LC3. *Methods Enzymol.* **452:**1–12; 2009.
[34] Ichimura, Y.; Komatsu, M. Selective degradation of p62 by autophagy. *Semin. Immunopathol.* **32:**431–436; 2010.
[35] Narendra, D.; Kane, L. A.; Hauser, D. N.; Fearnley, I. M.; Youle, R. J. p62/SQSTM1 is required for Parkin-induced mitochondrial clustering but not mitophagy; VDAC1 is dispensable for both. *Autophagy* **6:**1090–1106; 2010.
[36] Van Humbeeck, C.; Cornelissen, T.; Hofkens, H.; Mandemakers, W.; Gevaert, K.; De Strooper, B.; Vandenberghe, W. Parkin interacts with Ambra1 to induce mitophagy. *J. Neurosci.* **31:**10249–10261; 2011.
[37] Jing, E.; Emanuelli, B.; Hirschey, M. D.; Boucher, J.; Lee, K. Y.; Lombard, D.; Verdin, E. M.; Kahn, C. R. Sirtuin-3 (Sirt3) regulates skeletal muscle metabolism and insulin signaling via altered mitochondrial oxidation and reactive oxygen species production. *Proc. Natl. Acad. Sci. USA* **108:**14608–14613; 2011.
[38] Lopez-Lluch, G.; Irusta, P. M.; Navas, P.; de Cabo, R. Mitochondrial biogenesis and healthy aging. *Exp. Gerontol.* **43:**813–819; 2008.
[39] Nisoli, E.; Tonello, C.; Cardile, A.; Cozzi, V.; Bracale, R.; Tedesco, L.; Falcone, S.; Valerio, A.; Cantoni, O.; Clementi, E.; Moncada, S.; Carruba, M. O. Calorie restriction promotes mitochondrial biogenesis by inducing the expression of eNOS. *Science* **310:**314–317; 2005.
[40] Nisoli, E. Nitric oxide and mitochondrial biogenesis. *J. Cell Sci.* **119:**2855–2862; 2006.
[41] Cuervo, A. M.; Bergamini, E.; Brunk, U. T.; Droge, W.; Ffrench, M.; Terman, A. Autophagy and aging: the importance of maintaining "clean" cells. *Autophagy* **1:**131–140; 2005.
[42] Ballinger, S. W.; Patterson, C.; Yan, C. N.; Doan, R.; Burow, D. L.; Young, C. G.; Yakes, F. M.; Van Houten, B.; Ballinger, C. A.; Freeman, B. A.; Runge, M. S. Hydrogen peroxide- and peroxynitrite-induced mitochondrial DNA damage and dysfunction in vascular endothelial and smooth muscle cells. *Circ. Res.* **86:**960–966; 2000.
[43] Iwahara, T.; Bonasio, R.; Narendra, V.; Reinberg, D. SIRT3 functions in the nucleus in the control of stress-related gene expression. *Mol. Cell. Biol.* **32:**5022–5034; 2012.
[44] Olmos, Y.; Valle, I.; Borniquel, S.; Tierrez, A.; Soria, E.; Lamas, S.; Monsalve, M. Mutual dependence of Foxo3a and PGC-1alpha in the induction of oxidative stress genes. *J. Biol. Chem.* **284:**14476–14484; 2009.
[45] Chen, Z. H.; Yoshida, Y.; Saito, Y.; Niki, E. Adaptation to hydrogen peroxide enhances PC12 cell tolerance against oxidative damage. *Neurosci. Lett.* **383:**256–259; 2005.
[46] Franses, J. W.; Baker, A. B.; Chitalia, V. C.; Edelman, E. R. Stromal endothelial cells directly influence cancer progression. *Sci. Transl. Med.* **3:**66ra65; 2011.
[47] Avogaro, A.; de Kreutzenberg, S. V. Mechanisms of endothelial dysfunction in obesity. *Clin. Chim. Acta* **360:**9–26; 2005.
[48] Kim, J. A.; Wei, Y.; Sowers, J. R. Role of mitochondrial dysfunction in insulin resistance. *Circ. Res.* **102:**401–414; 2008.
[49] Dong, F.; Li, Q.; Sreejayan, N.; Nunn, J. M.; Ren, J. Metallothionein prevents high-fat diet induced cardiac contractile dysfunction: role of peroxisome proliferator activated receptor gamma coactivator 1alpha and mitochondrial biogenesis. *Diabetes* **56:**2201–2212; 2007.
[50] Choudhury, M.; Jonscher, K. R.; Friedman, J. E. Reduced mitochondrial function in obesity-associated fatty liver: SIRT3 takes on the fat. *Aging (Albany, NY)* **3:**175–178; 2011.
[51] Kleiner, S.; Mepani, R. J.; Laznik, D.; Ye, L.; Jurczak, M. J.; Jornayvaz, F. R.; Estall, J. L.; Chatterjee Bhowmick, D.; Shulman, G. I.; Spiegelman, B. M. Development of insulin resistance in mice lacking PGC-1alpha in adipose tissues. *Proc. Natl. Acad. Sci. USA* **109:**9635–9640; 2012.
[52] Ikemura, M.; Nishikawa, M.; Hyoudou, K.; Kobayashi, Y.; Yamashita, F.; Hashida, M. Improvement of insulin resistance by removal of systemic hydrogen peroxide by PEGylated catalase in obese mice. *Mol. Pharm.* **7:**2069–2076; 2010.